Social contagions on time-varying community networks

Mian-Xin Liu,[2,3] Wei Wang,[2,3,*] Ying Liu,[2,3,4] Ming Tang,[1,2,3,†] Shi-Min Cai,[2,3] and Hai-Feng Zhang[5]

[1]*School of Information Science Technology, East China Normal University, Shanghai 200241, People's Republic of China*

[2]*Web Sciences Center, University of Electronic Science and Technology of China, Chengdu 610054, People's Republic of China*

[3]*Big Data Research Center, University of Electronic Science and Technology of China, Chengdu 611731, People's Republic of China*

[4]*School of Computer Science, Southwest Petroleum University, Chengdu 610500, People's Republic of China*

[5]*School of Mathematical Science, Anhui University, Hefei 230601, People's Republic of China*

(Received 15 May 2016; revised manuscript received 4 March 2017; published 9 May 2017)

Time-varying community structures exist widely in real-world networks. However, previous studies on the dynamics of spreading seldom took this characteristic into account, especially those on social contagions. To study the effects of time-varying community structures on social contagions, we propose a non-Markovian social contagion model on time-varying community networks based on the activity-driven network model. A mean-field theory is developed to analyze the proposed model. Through theoretical analyses and numerical simulations, two hierarchical features of the behavior adoption processes are found. That is, when community strength is relatively large, the behavior can easily spread in one of the communities, while in the other community the spreading only occurs at higher behavioral information transmission rates. Meanwhile, in spatial-temporal evolution processes, hierarchical orders are observed for the behavior adoption. Moreover, under different information transmission rates, three distinctive patterns are demonstrated in the change of the whole network's final adoption proportion along with the growing community strength. Within a suitable range of transmission rate, an optimal community strength can be found that can maximize the final adoption proportion. Finally, compared with the average activity potential, the promoting or inhibiting of social contagions is much more influenced by the number of edges generated by active nodes.

DOI: 10.1103/PhysRevE.95.052306

I. INTRODUCTION

The dynamics of spreading is one of the hottest research topics in network science. The aim of this research is to reveal the underlying mechanisms in real spreading processes such as epidemic spreading, information spreading, behavior contagions, and innovation diffusion. The findings from it further provide theoretical supports for the forecasting and controlling of these spreading processes [1,2]. In general, based on the differences in the studied objects, the spreading processes can be classified into biological spreading and social contagions. The former focuses on the spreading of diseases or viruses on networks [3–6], while the latter focuses on contagions of information and behaviors on networks [7–10]. The social reinforcement effect in social contagions is the essential difference between biological spreading and social contagions [11]. It contains the idea that the adoption of an individual's behavior often depends on his neighbors' attitudes to the behavior [12,13]. For example, when an increasing number of our friends buy a new smartphone or watch a new movie, we are more likely to do so ourselves.

Previous research often focused on describing the influence of the social reinforcement effect on social contagions [12,14,15]. The Markovian linear threshold model is one of the most classical models studied [14]. In it, a non-adopter individual becomes an adopter once the number or proportion of his adopted neighbors exceeds a threshold. Watts found that the final behavior adoption proportion, following an increase in the average degree, first grows continuously and then decreases discontinuously [14]. However, an individual's decision to adopt a behavior not only depends on the *current state* of his neighbors, but it also relates to the behavioral information he has received *in the past*. The social reinforcement effect based on memory thus becomes an essential characteristic of social contagions. To describe the memory effect (or the so-called non-Markovian effect), Wang *et al.* proposed a social contagion model based on nonredundant memory information, and they found a continuous growth and a discontinuous growth of the behavior adoption proportion with the increasing information transmission rate [16,17]. They also found that an individual's limited contact capacity would reduce the final behavior adoption proportion [18].

However, most previous studies assumed that the network structures are unchanged. The latest empirical studies showed that in social networks the connections among individuals vary with time, which is not a feature of static networks [19]. The concept of time-varying networks (also be called as temporal network) was proposed to handle those real situations [20]. A widely observed phenomenon is that individuals are not always active in a social network due to limitations of time, funds, energy, or other resources. Perra *et al.* described these resources as the active potential of nodes, and they proposed an activity-driven network model that allows for an explicit representation of dynamical connectivity patterns [21]. At each time step, every individual becomes active or not according to its active potential. If an individual becomes active, it will randomly connect to some individuals. Spreading processes in an activity-driven network model show striking differences from the well-known results obtained in quenched and annealed networks [22]. Perra *et al.* found that the outbreak threshold of the SIS model on an activity-driven network is greater than that on the corresponding aggregated network [21].

*wwzqbx@hotmail.com

†tangminghan007@gmail.com

Liu *et al.* found that a disease spreads more slowly on activity-driven networks than it does on the corresponding aggregated networks, and the invasion threshold on the former is hundreds of times greater than that of the latter [23]. Holme *et al.* studied the threshold model on time-varying networks based on empirical data, and they found that the final adoption proportions increase due to the time-varying network structures [24].

Another significant feature observed in real-world networks is *community structure* [25,26], which can have a remarkable effect on the dynamics of spreading on networks. In previous studies, Liu *et al.* found that community structures can facilitate biological spreading on static networks [27], and Ahn *et al.* found that there is an optimal community strength that can greatly promote the social contagions [28]. Recent empirical studies showed that community structures also exist in time-varying networks [20,29]. However, the effects of these structures on social contagions are rarely discovered, and the exploration to them is still full of challenges. On the one hand, the contacts in time-varying networks vary over time and do not exist continuously. Thus, the spreading processes cannot be described accurately by the existing theoretical methods that succeeded in static networks. On the other hand, the mathematical analysis becomes much more complicated due to the non-Markovian and nonlinear characteristics of equations caused by strong social reinforcement effects.

In this paper, the effects of time-varying community structures on social contagions are systematically explored. First, a non-Markovian social contagion model on time-varying community networks is presented, and then a mean-field theory is developed. It is found that two hierarchical features exist in the behavior adoption processes: (i) when community strength is relatively large, the behavior can easily spread in one of the communities, while in the other community rapid spreading cannot occur until higher behavioral information transmission rates are adopted; (ii) hierarchical orders are displayed in the behavior adoption's spatial-temporal evolution patterns. Moreover, under different behavioral information transmission rates, along with the growth of community strength, three different growth patterns can be observed for the final behavior adoption proportion for the whole network. In a suitable transmission rate range, an optimal community strength that can maximize the final adoption proportion can be found. Lastly, it is found that the number of edges generated by active individuals plays a more important role in the promotion or inhibition of social contagions than the average activity potential.

II. MODELS

To study the effects of time-varying community networks on social contagions, a non-Markovian social contagion model on an activity-driven community network is proposed.

A. Activity-driven community network

In this section, we present a time-varying community network based on the activity-driven network model [21]. First, it is supposed that a network has N nodes (representing individuals), consisting of two communities A and B with equal sizes. Initially, each node is assigned with an equal activity potential a. Although it is hampered to some extent by the limitations of our results, we restrict ourselves here to a fixed a rather than the heterogeneous version [21] to simplify further analysis. The instantaneous network structure G_t is then generated as below: at a time step t, each node is activated with the probability a. If a node v is activated, it will generate m edges. Similar to the stochastic block model [30,31], each edge randomly connects to a node in the same community with a probability μ, called community strength, and to a node in the other community with a probability $1-\mu$ (as shown in Fig. 1). Multiple edges and self-loops are forbidden. To form community structures, we set $0.5 \leqslant \mu < 1$. There will be fewer edges between communities with the increase of μ. For a small value of μ, the community structure is not obvious. When $\mu = 0.5$, the probabilities of an edge connecting to the same or a different community are equal, and thus the time-varying community structures disappear. When $\mu = 1$, there is no edge between communities, which leads to two isolated networks. This case is meaningless and thus is excluded. At the end of time step t, all the generated edges are

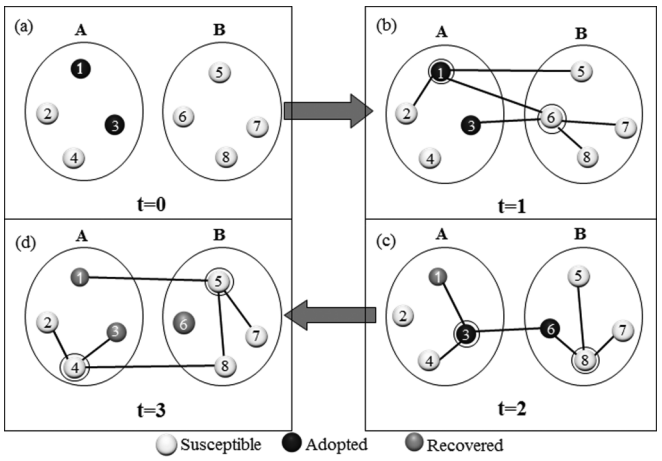

FIG. 1. An illustration of the social contagion model on an activity-driven community network. The network is divided into two equal-sized communities A and B, each with four nodes. The circle around a node indicates that the node is active. (a) At $t = 0$, nodes 1 and 3 are randomly selected as seeds on community A, and the remaining nodes are susceptible. (b) At $t = 1$, the instantaneous structure G_1 is generated, in which nodes 1 and 6 are activated with probability $a = 0.25$, and $m = 3$ edges are generated. Every edge connects to nodes in the same community with probability $u = 0.6$ and with probability $1 - u = 0.4$ to the other community. Adopted nodes 1 and 3 transmit the behavioral information to their susceptible neighbors with $\lambda = 0.8$. Note that node three transmits the information without activation. Node 6 receives two pieces of information, which reach the adoption threshold $\pi = 2$, and thus it becomes adopted. Then, nodes 1 and 3 try to become recovered with $\gamma = 0.1$. Finally, delete all edges generated at this time step. (c) At $t = 2$, nodes 3 and 8 become active and form the instantaneous structure G_2. No information transmission succeeds this time. Then nodes 3 and 6 both become recovered successfully. (d) At $t = 3$, nodes 4 and 5 are activated in the instantaneous structure G_3. The contagion process terminates since all adopted nodes become recovered.

deleted. A time-varying community network is generated by repeating the above process.

B. Social contagion model

In this section, a non-Markovian model, called the susceptible-adopted-recovered (SAR) model, is proposed to describe a social contagion on time-varying community networks [16,32]. The states of the nodes are divided into susceptible, adopted, and recovered. In the susceptible state a node has not adopted the behavior, and it is willing to receive behavioral information from its neighbors who have adopted the behavior. In the adopted state a node has adopted the behavior, and it is willing to spread the behavioral information to its neighbors. In the recovered state a node loses interest in the behavior and no longer anticipates the spreading process. Each node holds a constant adoption threshold π, which reflects its will to adopt the behavior. In addition, a memory variable χ_i represents how many pieces of behavioral information node i has received. By introducing χ_i, the dynamics of the social contagion essentially becomes non-Markovian.

In the beginning, a proportion ρ_0 of nodes are randomly chosen as seeds (initial adopters), and the remaining nodes are susceptible. A synchronous updating method is adopted to update the nodes' states [16]. At each time step, an instantaneous structure G_t is first generated according to the method described in Sec. II A. Then the behavior spreads on network G_t as follows. Every adopted node (not only active nodes) v transmits the behavioral information to each susceptible neighbor u in G_t with the probability λ. If u receives the information successfully, its memory variable χ_u will be increased by 1. If χ_u reaches or exceeds the adoption threshold π, the node u will become adopted. Note that if $\pi = 1$, the model is memoryless, and thus we only discuss the situation of $\pi > 1$. At the same time step, the adopted nodes become recovered with probability γ. The contagion process terminates once all adopted nodes are recovered. In this model, the probabilities λ and γ can be interpreted as the transmission rate and the recovery rate, respectively. Contrary to the model in [16], in which the redundant information is not allowed to transmit between two individuals, our proposed model allows a pair of individuals to transmit the same message repeatedly. An illustration of our model is provided in Fig. 1.

III. THEORY

In the section, a mean-field approximation theory is developed to describe quantitatively the non-Markovian social contagions on a time-varying community network. In this theory, the network size is assumed to be very large, i.e., $N \to \infty$ in the thermodynamic limit.

The degree distribution of the time-varying community network should be derived first. Although the edges are changing with time, we can still capture the degree distribution of the instantaneous structure G_t. There are two types of nodes in G_t, namely active nodes and inactive nodes. The inactive nodes are unable to generate edges, but they can receive connections from active nodes. Based on the definitions of m and a described in Sec. II A, it is expected that Nma edges

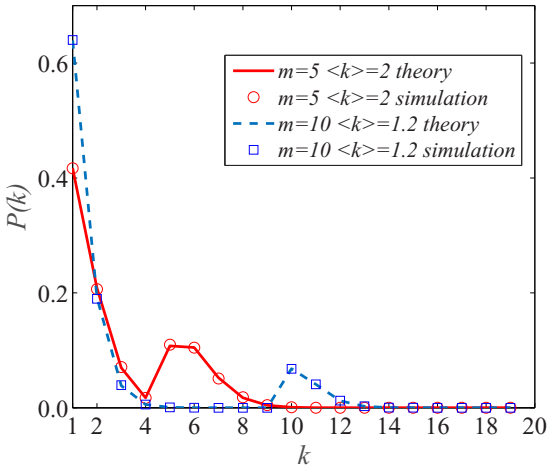

FIG. 2. The degree distributions of the instantaneous structure obtained from numerical simulations and theoretical predictions. The solid line (circles) and the dashed line (squares) represent the theoretical predictions (simulation results) of degree distribution with $m = 5, \langle k \rangle = 2$ and $m = 10, \langle k \rangle = 1.2$, respectively. Other parameters are set to be $N = 10\,000$, $\mu = 0.8$. The simulation results are averaged over 1000 realizations. All presented results have been normalized within the range $1 \leqslant k < 20$.

exist in G_t. In the community network, two communities are of the same size, and each generated edge may connect from an active node to a node in the same (or different) community with the probability $\mu/(N/2-1)$ [or $(1-\mu)/(N/2)$]. Thus, every node has the same probability of about $1/N$ to receive a connection. The probability that an inactive node has degree k is

$$P_I(k) = \binom{maN}{k}\left(\frac{1}{N}\right)^k\left(1-\frac{1}{N}\right)^{maN-k}. \tag{1}$$

In the thermodynamic limit, i.e., $N \to \infty$, maN is very large and $1/N$ is quite small. We can rewrite Eq. (1) as

$$P_I(k) = \frac{(ma)^k}{k!}e^{-ma}. \tag{2}$$

For an active node with degree k, it generates m edges toward other nodes, and $k-m$ edges are received from other active nodes. Similarly, we get the degree distribution $P_A(k)$ of active nodes as

$$P_A(k) = \begin{cases} 0 & \text{if } k < m, \\ \frac{(ma)^{k-m}}{(k-m)!}e^{-ma} & \text{if } k \geqslant m. \end{cases} \tag{3}$$

Combining Eqs. (2) and (3), the instantaneous degree distribution for the time-varying network G_t is

$$P(k) = (1-a)P_I(k) + aP_A(k). \tag{4}$$

In Fig. 2, it is shown that our approximation works quite well even when the community strength is relatively large ($\mu = 0.8$) or when the averaged degree is not an integer ($\langle k \rangle = 2ma = 1.2$).

We next discuss the situations within and between communities. Only the theoretical analysis of community A will be introduced in detail, since the results on community B can be derived simply by exchanging the indexes "A" and "B."

A node v_A belonging to community A connects to nodes in the same community with probability μ and to nodes in a different community with probability $1-\mu$. Therefore, the probability of node v_A with degree k connecting to i nodes in community A can be easily written as

$$\omega^{AA}(k,i) = P(k)\binom{k}{i}\mu^i(1-\mu)^{k-i}, \tag{5}$$

and in community B the form is given as

$$\omega^{AB}(k,i) = P(k)\binom{k}{i}(1-\mu)^i\mu^{k-i}, \tag{6}$$

where $i = 0,1,\ldots,k$.

After analyzing the network structure, we turn to describe social contagions. We denote the proportion of susceptible nodes who have received r pieces of behavioral information in community A and community B at time step t as $S_A(r,t)$ and $S_B(r,t)$, respectively. $\rho_A(t)$ and $\rho_B(t)$ are used to denote the proportion of adopted nodes in communities A and B, respectively, and $R_A(t)$ and $R_B(t)$ are used to denote the proportion of recovered nodes at time step t. When $t \to \infty$, all adopted nodes become recovered. We denote the final proportion of nodes in the recovered state in communities A and B ($N/2$ nodes) as $R_A(\infty)$ and $R_B(\infty)$, respectively. The final behavior adoption proportion in the whole network (N nodes) is computed as $R(\infty) = [R_A(\infty) + R_B(\infty)]/2$.

To write the equations for the time evolution of each type of node, we must first know the probability that v_A has n adopted neighbors at time step t, denoted as $\theta^A(n,t)$. Suppose v_A has i neighbors in community A in the instantaneous structure G_t [see Eq. (5)]. The probability that j nodes of these i neighbors are in an adopted state is

$$\xi_{AA}(i,j,t) = \binom{i}{j}[\rho_A(t)]^j[1-\rho_A(t)]^{i-j}. \tag{7}$$

Similarly, the probability that v_A with i neighbors in community B and j of them are adopted is given by

$$\xi_{AB}(i,j,t) = \binom{i}{j}[\rho_B(t)]^j[1-\rho_B(t)]^{i-j}. \tag{8}$$

Notice that $\omega^{AA}(k,i)$ also means the probability that v_A, given degree k, connects to $k-i$ nodes in community B for the above inference, that is to say, $\omega^{AA}(k,i) = \omega^{AB}(k,k-i)$. We have the probability that the v_A connects to n adopted neighbors in the whole network,

$$\theta^A(n,t) = \sum_{k=1}^{k_{\max}}\sum_{i=0}^{k}\omega^{AA}(k,i)\sum_{j=0}^{\min(n,i)}[\xi_{AA}(i,j,t) \times \xi_{AB}(k-i,n-j,t)], \tag{9}$$

where $\min(x,y)$, denoting the minimum value of x and y, is used to avoid the situations that j exceeds i or n. For a susceptible node v_A with n adopted neighbors at time step t, the probability that it receives at least one piece of behavioral information from its neighbors is

$$\psi_A(t) = \sum_{n=1}^{k_{\max}}\theta_A(n,t)[1-(1-\lambda)^n]. \tag{10}$$

Note that we should sum up all possible values of k to the maximum degree $k_{\max}$ when numerically solving the equations. Similarly, the probability that v_A receives $i \geqslant 1$ pieces of behavioral information can be expressed as

$$\phi_A(i,t) = \sum_{n=i}^{k_{\max}}\theta_A(n,t)\binom{n}{i}\lambda^i(1-\lambda)^{n-i}. \tag{11}$$

Obviously, Eq. (10) can be derived by Eq. (11) as

$$\psi_A(t) = \sum_{i=1}^{k_{\max}}\phi_A(i,t). \tag{12}$$

The time evolution of the contagion process can be described by a developed mean-field approximation. For $S_A(r,t)$ $(r=0)$, the nodes that have not received any behavioral information at time step t will change into other states when they receive at least one piece of behavioral information. Denote the proportion of these nodes as $S_A(0,t)$, and yield

$$\frac{dS_A(0,t)}{dt} = -S_A(0,t)\psi_A(t). \tag{13}$$

For $1 \leqslant r < \pi$, the change of $S_A(r,t)$ is induced by two cases. $S_A(r,t)$ increases when the nodes who have only received fewer than r pieces of behavioral information, whose proportion is $S_A(q,t)$ $(0 \leqslant q < r)$, receive $r-q$ pieces of behavioral information with probability $\sum_{q=0}^{r-1}S_A(q,t)\phi_A(r-q,t)$. At the same time, $S_A(r,t)$ decreases because those nodes with r pieces of behavioral information receive at least one piece of information and turn to other states with the probability $S_A(r,t)\psi_A(t)$. The evolution equation of $S_A(r,t)$ can be written as

$$\frac{dS_A(r,t)}{dt} = \sum_{q=0}^{r-1}S_A(q,t)\phi_A(r-q,t) - S_A(r,t)\psi_A(t). \tag{14}$$

Similarly, the increase of adopted nodes results from the state change of susceptible nodes who have received information being equal to or over the threshold π, with probability $\sum_{q=0}^{\pi-1}S_A(q,t)[\psi_A(t) - \sum_{i=1}^{\pi-1-q}\phi_A(i,t)]$, and the decrease is due to their recovery, with probability $\gamma\rho_A(t)$. Thus the evolution of the proportions of adopted and recovered nodes can be written as

$$\frac{d\rho_A(t)}{dt} = \sum_{q=0}^{\pi-1}S_A(q,t)\left[\psi_A(t) - \sum_{i=1}^{\pi-1-q}\phi_A(i,t)\right] - \gamma\rho_A(t) \tag{15}$$

and

$$\frac{dR_A(t)}{dt} = \gamma\rho_A(t), \tag{16}$$

respectively.

Now, Eqs. (13)–(16) form a complete description of the social contagions process, allowing us to compute the proportion of nodes in any state in community A at any time step. By transferring our knowledge to community B, the time evolutions in community B can be obtained.

The outbreak threshold of social contagion λ_c is a crucial physical parameter. When the information transmission rate λ

is greater than λ_c, a finite fraction of nodes will adopt the behavior. When $\lambda \leqslant \lambda_c$, there is only a vanishingly small fraction of nodes adopting the behavior. Initially, there are few nodes in the adopted state, thus $S_A(0) \to 1$, $S_B(0) \to 1$, $\rho_A(0) \to 0$, $\rho_B(0) \to 0$, $R_A(0) \to 0$, and $R_B(0) \to 0$. Previous studies indicated that the behavior can break out over the network if and only if the proportion of adopted individuals can grow exponentially at the initial time [33,34]. Thus, one expects to obtain λ_c by analyzing the stability around $S_A(0) \to 1$. Unfortunately, this method is not suitable for our model because of the following two reasons. On the one hand, a vanishingly small fraction of initial adopters cannot lead to the quick growth of adoption at the initial time in our model, as the susceptible nodes cannot immediately accumulate the information memory to reach or exceed the adoption threshold π [16]. To this extent, $S_A(0) \to 1$ might not be a feasible fix point. On the other hand, the nonlinearity out of the memory effects in the system makes the linearization method near the stability point ineffective [35]. Therefore, the outbreak threshold cannot be obtained by the linearization method. To get the outbreak threshold, further research is needed.

IV. SIMULATION RESULTS

Based on the proposed model, we perform extensive simulations to investigate the social contagions on time-varying community networks. In the simulations, the size of network, the recovery probability, adoption threshold, and the initial adopter proportion are set to be $N = 10\,000$, $\gamma = 0.1$, $\pi = 3$, and $\rho_0 = 0.03$, respectively. In the beginning, $N\rho_0$ nodes in community A are randomly chosen as seeds of the adopter, and the remaining nodes in the whole network are susceptible. The simulation results of the final adoption proportion (FAP) $R_A(\infty)$, $R_B(\infty)$, and $R(\infty)$ are obtained by averaging the results over 2000 independent realizations. The theoretical values of $R_A(\infty)$, $R_B(\infty)$, and $R(\infty)$ are given by solving Eqs. (13)–(16). In the following subsections, the effects of community structure and time-varying structure on social contagions will be discussed separately.

A. Effects of community structure

We first explore the growths of $R_A(\infty)$, $R_B(\infty)$, and $R(\infty)$ versus the information transform rate λ under different community strength μ. Different growth patterns can be observed in Fig. 3. For relatively small μ (0.5 and 0.9), nodes in community A and B start to adopt the behavior almost at the same λ [see Figs. 3(a) and 3(b)]. This is because the effect of community structure is not obvious when μ is small, and the adopted nodes are able to transmit the behavioral information across the community. However, for relatively large values of μ (0.95 and 0.97), a hierarchical feature arises in the behavior adoption process: nodes in community A begin to adopt the behavior at small λ, while the adoption in community B does not occur until λ reaches a larger value [Figs. 3(c) and 3(d)]. In this situation, nodes tend to transmit information to nodes in the same community, which makes it difficult to transmit the information to community B and thus leads to the hierarchy mentioned above. The

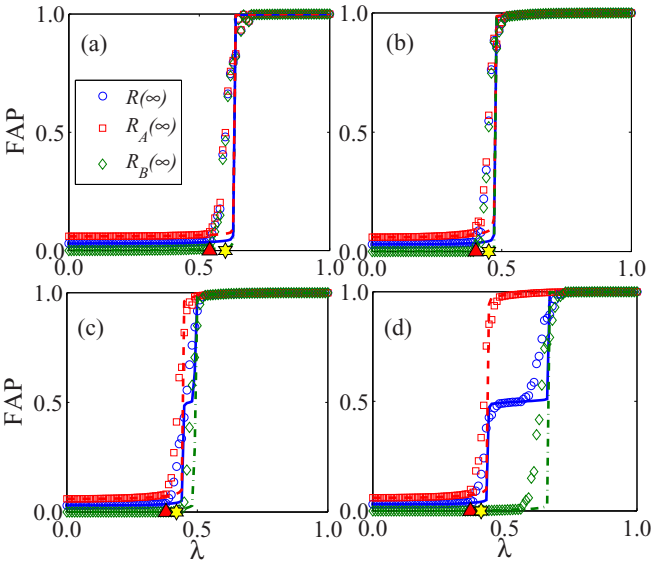

FIG. 3. The final adoption proportion (FAP) $R(\infty)$, $R_A(\infty)$, and $R_B(\infty)$ vs information transmission probability λ under different community strengths. In the figure, (a) $\mu = 0.5$, (b) $\mu = 0.9$, (c) $\mu = 0.95$, and (d) $\mu = 0.97$. The solid line (circles), dashed line (squares), and dotted line (diamonds) represent the theoretical predictions (simulation results) of $R(\infty)$, $R_A(\infty)$, and $R_B(\infty)$, respectively. Simulation and theoretical suggested outbreak thresholds λ_c are labeled by triangles and stars, which are recorded as soon as $R(\infty)$ is slightly larger than ρ_0, that is, $R(\infty) > 0.04$, due to the difficulty of determining the outbreak threshold [38,39]. The suggested thresholds are (a) $\lambda_c = 0.54, 0.60$; (b) $\lambda_c = 0.40, 0.44$; (c) $\lambda_c = 0.38, 0.42$; and (d) $\lambda_c = 0.37, 0.41$ for simulation and theoretical results, respectively. Other parameters are set to be $N = 10\,000$, $\rho_0 = 0.03$, $a = 0.2$, $m = 5$, $\gamma = 0.1$, and $\pi = 3$, respectively.

theoretical predictions give a quantitative description of the above phenomena, which are basically in agreement with the simulation results, including the suggested outbreak threshold λ_c. The deviations between the theoretical predictions and the simulation results could be explained by the dynamical correlations among neighbors and finite-size network effects [36,37]. Figure 4 displays the growth patterns of $\rho_A(t)$ and

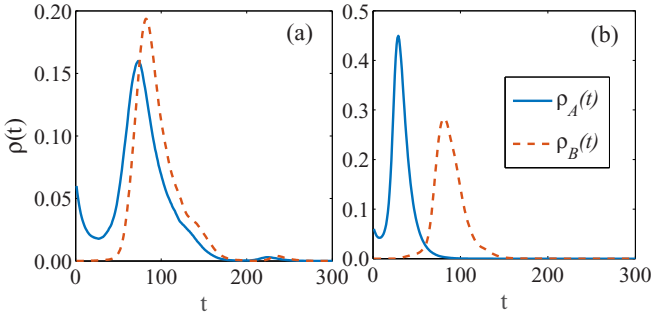

FIG. 4. Time evolutions of $\rho_A(t)$ and $\rho_B(t)$, in which (a) and (b) correspond to Figs. 3(b) and 3(d), respectively. The time series shown above are sampled under parameters $\lambda = 0.6$ and time span [0,300], and they are averaged over 200 realizations. The remaining parameters are set to be the same as those in Figs. 3(b) and 3(d).

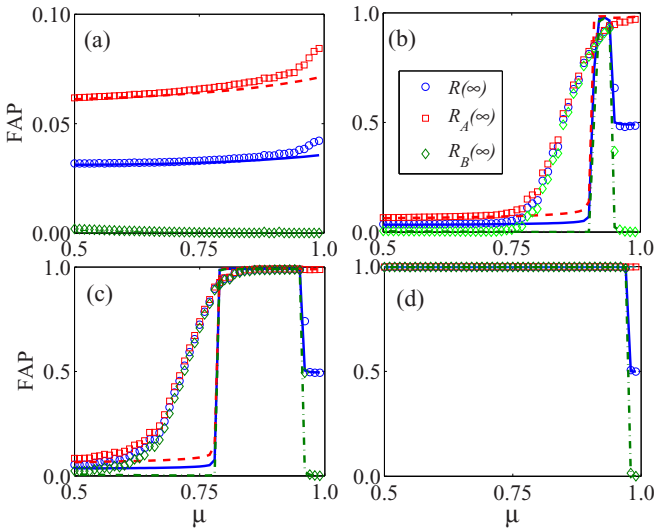

FIG. 5. The FAP $R(\infty)$, $R_A(\infty)$, and $R_B(\infty)$ vs community strength μ under different information transmission rates (a) $\lambda = 0.35$, (b) $\lambda = 0.47$, (c) $\lambda = 0.55$, and (d) $\lambda = 0.7$. The solid line (circles), dashed line (squares), and dotted line (diamonds) represent the theoretical values (simulation values) of $R(\infty)$, $R_A(\infty)$, and $R_B(\infty)$, respectively. Other parameters are set to be the same as in Fig. 3.

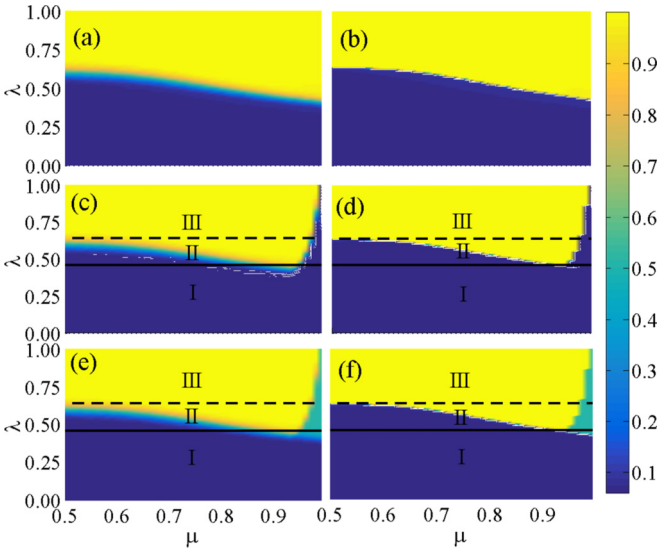

FIG. 6. The FAP $R_A(\infty)$, $R_B(\infty)$, and $R(\infty)$ vs community strength μ and information transmission rate λ. Color-coded values show simulation results in (a) $R_A(\infty)$, (c) $R_B(\infty)$, and (e) $R(\infty)$, and theoretical predictions in (b) $R_A(\infty)$, (d) $R_B(\infty)$, and (f) $R(\infty)$, respectively. Other parameters are set to be the same as in Fig. 3.

$\rho_B(t)$ versus time t, respectively, corresponding to the cases in Figs. 3(b) and 3(d). Actually, another hierarchical feature is displayed in Fig. 3, from which it can be observed that the increase of $\rho_A(t)$ and $\rho_B(t)$ actually starts at different times. We call this the spatial-temporal hierarchy due to the spatial-temporal order exhibited in the contagions processes. We stress the differences between the two hierarchies because under the same parameters, Fig. 4(a) shows two separate peaks that might indicate divergence in the time order of outbreaks, while Fig. 3(b) exhibits no obvious feature to identify the hierarchy. Thus, it can be concluded that they are two independent phenomena.

Figure 5 provides the growths of $R_A(\infty)$, $R_B(\infty)$, and $R(\infty)$ versus μ under different λ. Three different growth patterns can be observed. For small values of λ in Fig. 5(a), $R(\infty)$, $R_A(\infty)$, and $R_B(\infty)$ increase monotonically with growing μ. The λ range showing this phenomenon is called as the *enhancing-only* region. With the increase of λ, as shown in Figs. 5(b) and 5(c), $R_A(\infty)$ increases with μ monotonically, while $R_B(\infty)$ and $R(\infty)$ first rise and then decline. The peaks in Figs. 5(b) and 5(c) indicate the existence of the optimal community strength promoting the behavior adoption. We identify this λ range as the *enhancing-depressing* region. The optimal contagion phenomenon can be explained as follows: there are more edges in the community for larger μ, which promotes the information spreading within community A. Meanwhile, the number of bridge edges between communities decreases with growing μ. If μ is large enough, the global behavior adoption will be inhibited, resulting in a decrease of $R_B(\infty)$ and $R(\infty)$. When λ is very large, nodes in both communities adopt the behavior easily [as shown in Fig. 5(d)]. For any given μ, the $R_A(\infty)$ can always reach a large value. When μ is large enough, the two communities tend to be isolated and the global behavior adoption will be suppressed, leading to a decrease of $R_B(\infty)$ and $R(\infty)$. Thus, this range of large λ is regarded as the *depressing-only* region. It is noted that the optimal contagion phenomena occur near the outbreak threshold λ_c (refer to Fig. 6 later), so there are slightly obvious deviations between the theoretical predictions and the simulation results in Figs. 5(b) and 5(c).

Figure 6 also presents a whole picture of the effects of λ and μ on $R_A(\infty)$, $R_B(\infty)$, and $R(\infty)$. According to the definitions in the preceding paragraph, the (μ,λ) planes are divided into three regions: (i) the enhancing-only region, (ii) the enhancing-depressing region, and (iii) the depressing-only region. As $R_A(\infty)$ increases monotonically with μ, only region I exists in Figs. 6(a) and 6(b). Due to the effect of time-varying community structures, three different regions can be observed in Figs. 6(c)–6(f). This means that there exists an optimal community strength within a certain range of λ that can help the values of $R_B(\infty)$ and $R(\infty)$ reach their maximum values. As shown in Figs. 6(b), 6(d), and 6(f), the theoretical results fit the simulation results illustrated in Figs. 6(a), 6(c), and 6(e).

B. Effect of time-varying structure

In Fig. 7, the effect of time-varying structure on social contagions is investigated. According to the description of the time-varying community structure, the average degree of G_t is $\langle k \rangle = 2ma$ at time step t, which allows us to compare the relative importance of time-varying structure parameters m and a on the social contagions. Keeping the remaining parameters the same as Fig. 3, we fix the average degree $\langle k \rangle = 2$, and we adjust the values of m and a. To draw Fig. 7, the contour plots of certain $R(\infty)$ are obtained in the parameter plane (μ,λ) with different values of m and a. The contours with $R(\infty) = 0.4$ and 0.7 are demonstrated in Figs. 7(a) and 7(b),

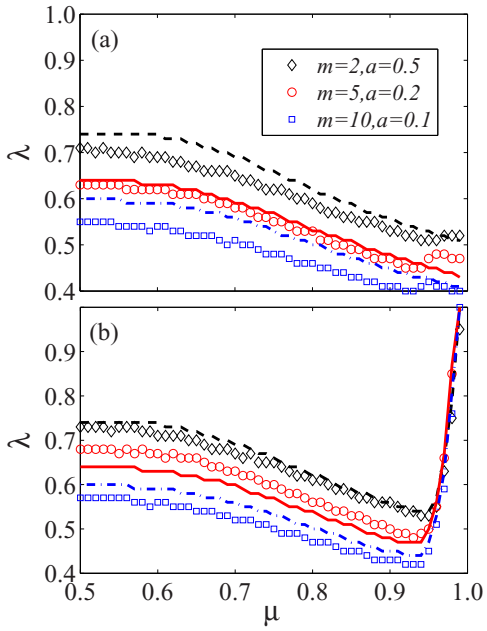

FIG. 7. The behavioral information transmission rate λ vs community strength μ for a given FAP (a) $R(\infty) = 0.4$ and (b) $R(\infty) = 0.7$. The dashed line (diamonds), solid line (circles), and dotted line (squares) denote the theoretical values (simulation values) of $m = 2$, $a = 0.5$; $m = 5$, $a = 0.2$; and $m = 10$, $a = 0.1$, respectively. Other parameters are set to be of $N = 10\,000$, $\rho_0 = 0.03$, $\gamma = 0.1$, and $\pi = 3$, respectively.

respectively. With these contours, the corresponding values of λ for a given $R(\infty)$ and μ can be visualized. The change in the corresponding value of λ actually reflects whether the social contagions are promoted or inhibited. For example, if the corresponding value of λ become lower, it can be known that the social contagions are promoted, because it is easier to reach the given $R(\infty)$ under some μ. Based on this, one can expect that if the importance of m and a is equal, when they change inversely proportional to each other their influences on social contagions will counteract with each other, and the contours of simulation results and theoretical solutions will remain almost the same.

However, as shown in Fig. 7, the contours move down obviously with the increase of m/a, which implies that the influences of m actually exceed the influences of a. The phenomenon can be explained in the following way: increasing the value of m/a means decreasing the number of active nodes and increasing the average degree of active nodes, which leads to the emergence of active nodes with a large degree. When active nodes have a large degree, they will have a high probability to get in touch with adopted nodes and become adopted at one time step, thus these contacts are effective. On the contrary, small m/a will result in a small degree of active nodes in an instantaneous structure. These active nodes will not receive enough information at one time step, and they wait for another round of activation. During the resting, the adopters in the network might be recovered. Thus, though the number of active nodes existing at one step is reduced because of the small value of a, their large degrees still make contacts efficient, and thus $R(\infty)$ can reach the assigned value more easily. To this extent, compared with the parameter a, parameter m has a more crucial influence on promoting or inhibiting the social contagions.

For other average degrees, such as $\langle k \rangle = 0.2, 1, 3$, similar phenomena can be observed. The results from our theoretical method display similar phenomena about the effects of m/a in Fig. 7.

V. DISCUSSION

In this paper, the goal of which was to explore the effects of time-varying community structures on social contagions, and we proposed a non-Markovian social contagion model on a time-varying community network. We then developed the mean-field theory to quantitatively describe the proposed model. Through theoretical analysis and extensive numerical simulations, it is shown that there are two hierarchical features in the behavior adoption processes. In one regard, the behavior spreads in one of the communities easily, while a larger information transmission rate is required for outbreak in the other community. Independently, the behavior adoption displays a hierarchical feature in the spatial-temporal evolution pattern. Moreover, under different behavioral information transmission rates, the final behavior adoption proportion in the whole network versus the community strength can show one of the different patterns, i.e., the enhancing-only pattern, the enhancing-depressing pattern, or the depressing-only pattern. In the enhancing-depressing region, optimal community strength can be easily found, at which the final adoption proportion is maximized. Finally, we discovered that the number of edges generated by active individuals plays a more important role on social contagions than the average activity potential. In general, our developed theory succeeded in qualitatively predicting the occurrence of various phenomena in simulations, though a more accurate theoretical approach is urgently needed.

This work can help us to better understand, predict, and control social contagions on social networks. However, we assumed that all individuals have the same activity potential. The role of heterogeneous activity potentials should be addressed in future studies, e.g., by using activity potentials with power-law distribution. To distinguish the difference between time-varying networks and static networks, a comparable static network model should be carefully designed. In addition, the effect of social contagions on epidemic spreading and the relationship between time-varying networks and multilayer networks are worthy of future study [40–44].

ACKNOWLEDGMENTS

This work was supported by the National Natural Science Foundation of China under Grants No. 11575041, No. 11105025, No. 61673086, and No. 61473001, the Fundamental Research Funds for the Central Universities (Grant No. ZYGX2015J153), and the Scientific Research Starting Program of Southwest Petroleum University (Grant No. 2014QHZ024).

[1] R. Pastor-Satorras, C. Castellano, P. Van Mieghem, and A. Vespignani, Rev. Mod. Phys. **87**, 925 (2015).
[2] W. Wang, M. Tang, H. E. Stanley, and L. A. Braunstein, Rep. Prog. Phys. **80**, 036603 (2017).
[3] C. Granell, S. Gómez, and A. Arenas, Phys. Rev. Lett. **111**, 128701 (2013).
[4] M. E. J. Newman, Phys. Rev. E **66**, 016128 (2002).
[5] T. Gross, C. J. D. D'Lima, and B. Blasius, Phys. Rev. Lett. **96**, 208701 (2006).
[6] M. Small, D. M. Walker, and C. K. Tse, Phys. Rev. Lett. **99**, 188702 (2007).
[7] H. P. Young, Proc. Natl. Acad. Sci. USA **108**, 21285 (2011).
[8] D. Centola, Science **334**, 1269 (2011).
[9] A. D. Kramer, J. E. Guillory, and J. T. Hancock, Proc. Natl. Acad. Sci. USA **111**, 8788 (2014).
[10] J. P. Gleeson, K. P. O'Sullivan, R. A. Baños, and Y. Moreno, Phys. Rev. X **6**, 021019 (2016).
[11] C. Castellano, S. Fortunato, and S. Fortunato, Rev. Mod. Phys. **81**, 591 (2009).
[12] P. S. Dodds and D. J. Watts, Phys. Rev. Lett. **92**, 218701 (2004).
[13] P. S. Dodds and D. J. Watts, J. Theor. Biol. **232**, 587 (2005).
[14] D. J. Watts, Proc. Natl. Acad. Sci. USA **99**, 5766 (2002).
[15] D. Centola, Science **329**, 1194 (2010).
[16] W. Wang, M. Tang, H. F. Zhang, and Y. C. Lai, Phys. Rev. E **92**, 012820 (2015).
[17] W. Wang, M. Tang, P. Shu, and Z. Wang, New J. Phys. **18**, 013029 (2016).
[18] W. Wang, P. Shu, Y. X. Zhu, M. Tang, and Y. C. Zhang, Chaos **25**, 103102 (2015).
[19] P. Holme and J. Saramäki, *Temporal Networks* (Springer, Berlin, 2013).
[20] P. Holme and J. Saramäki, Phys. Rep. **519**, 97 (2012).
[21] N. Perra, B. Gonçalves, R. Pastor-Satorras, and A. Vespignani, Sci. Rep. **2**, 469 (2012).
[22] N. Perra, A. Baronchelli, D. Mocanu, B. Gonçalves, R. Pastor-Satorras, and A. Vespignani, Phys. Rev. Lett. **109**, 238701 (2012).
[23] S. Y. Liu, A. Baronchelli, and N. Perra, Phys. Rev. E **87**, 032805 (2013).
[24] F. Karimi and P. Holme, Physica A **392**, 3476 (2013).
[25] M. Girvan and M. E. J. Newman, Proc. Natl. Acad. Sci. USA **99**, 7821 (2002).
[26] M. E. J. Newman, Proc. Natl. Acad. Sci. USA **103**, 8577 (2006).
[27] Z. H. Liu and B. Hu, Europhys. Lett. **72**, 315 (2005).
[28] A. Nematzadeh, E. Ferrara, A. Flammini, and Y. Y. Ahn, Phys. Rev. Lett. **113**, 088701 (2014).
[29] P. J. Mucha, R. Thomas, K. Macon, M. A. Porter, and J. P. Onnela, Science **328**, 876 (2012).
[30] B. Karrer and M. E. J. Newman, Phys. Rev. E **83**, 016107 (2011).
[31] B. Ball, B. Karrer, and M. E. J. Newman, Phys. Rev. E **84**, 036103 (2011).
[32] P. Shu, W. Wang, M. Tang, P. Zhao, and Y. C. Zhang, Chaos **26**, 063108 (2016).
[33] W. Wang, M. Tang, H. Yang, Y. Do, Y. C. Lai, and G. W. Lee, Sci. Rep. **4**, 5097 (2014).
[34] M. E. J. Newman, *Networks An Introduction* (Oxford University Press, Oxford, 2010).
[35] F. Radicchi, Nat. Phys. **11**, 597 (2015).
[36] F. J. Pérez-Reche, J. J. Ludlam, S. N. Taraskin, and C. A. Gilligan, Phys. Rev. Lett. **106**, 218701 (2011).
[37] P. B. Cui, M. Tang, and Z. X. Wu, Sci. Rep. **4**, 6303 (2014).
[38] L. Ferreri, P. Bajardi, M. Giacobini, S. Perazzo, and E. Venturino, Phys. Rev. E **90**, 012812 (2014).
[39] Q. H. Liu, W. Wang, M. Tang, and H. F. Zhang, Sci. Rep. **6**, 25617 (2016).
[40] Z. Y. Ruan, M. Tang, and Z. H. Liu, Phys. Rev. E **86**, 036117 (2012).
[41] H. X. Yang, M. Tang, and Y. C. Lai, Phys. Rev. E **91**, 062817 (2015).
[42] A. Saumell-Mendiola, M. Á. Serrano, and M. Boguná, Phys. Rev. E **86**, 026106 (2012).
[43] A. Arenas, A. Díaz-Guilera, and R. Guimerà, Phys. Rev. Lett. **86**, 3196 (2001).
[44] M. Kivela, A. Arenas, M. Barthelemy, J. P. Gleeson, Y. Moreno, and M. Porter, J. Complex Netw. **2**, 203 (2014).